JCTC Journal of Chemical Theory and Computation

Article

pubs.acs.org/JCTC

The Nature of Transannular Interactions in E_4N_4 and E_8^{2+} (E = S, Se)

Jani Moilanen,[†] Antti J. Karttunen,[†] Heikki M. Tuononen,*[,†] and Tristram Chivers*[,‡]

[†]Department of Chemistry, P.O. Box 35, FI-40014 University of Jyväskylä, Finland

[‡]Department of Chemistry, University of Calgary, Calgary, AB, T2N 1N4, Canada

Supporting Information

ABSTRACT: The electronic structures of tetrachalcogen tetranitrides, E_4N_4, and octachalcogen dications, E_8^{2+}, and the nature of their *intramolecular* E···E interactions (E = S, Se) was studied with high-level theoretical methods. The results reveal that the singlet ground states of both systems have a surprisingly large correlation contribution which functions to weaken and therefore lengthen the cross-ring E−E bond. The observed correlation effects are primarily static in E_4N_4, whereas in E_8^{2+} the dynamic part largely governs the total correlation contribution. The presented description of bonding is the first that gives an all-inclusive picture of the origin of cross-ring interactions in E_4N_4 and E_8^{2+}; not only does it succeed in reproducing all experimental structures but it also offers a solid explanation for the sporadic performance of different computational methods that has been reported in previous studies. Furthermore, the theoretical data demonstrate that E···E bonds in E_4N_4 and E_8^{2+} are unique and fundamentally different from, for example, dispersion that plays a major role in weak *intermolecular* chalcogen···chalcogen contacts.

INTRODUCTION

Weak transannular chalcogen···chalcogen interactions are a recurring theme in the chemistry of certain electron-rich inorganic heterocycles.[1] Tetrasulfur tetranitride (**1a**) is an archetypical member of this group:[2] S_4N_4 has a cage-like structure with two short intramolecular S···S interactions as determined by single crystal X-ray diffraction (Figure 1).[3−5]

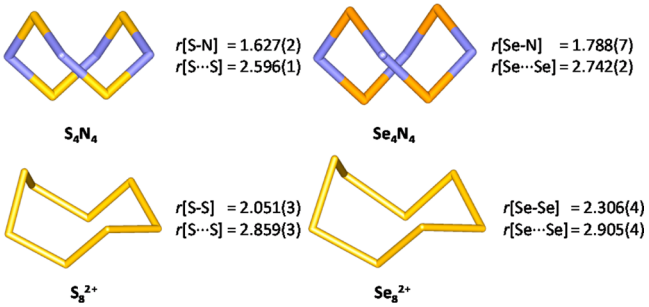

Figure 1. Experimental X-ray structures of E_4N_4 and E_8^{2+} (E = S, Se). Average bond lengths are given in Ångströms.[5,7,8,17,19]

The selenium analogue of **1a** is also known (**1b**),[6−8] as is the hybrid species $S_2Se_2N_4$ (**1c**),[9] and they are both structurally isomorphous with S_4N_4. Other cyclic species with a single transannular chalcogen···chalcogen interaction can be obtained from **1a** when its two antipodal sulfur atoms are replaced by a group that formally contributes one valence electron less to the system. For example, S ⇒ CR and S ⇒ PR_2 substitutions afford dithiatetrazocines $RC(NSN)_2CR$ (**2**;[10] R = NMe_2) and diphosphadithiatetrazocines $R_2P(NSN)_2PR_2$ (**3**; R = Me, Et, Ph, Cl),[11−14] respectively, with a bicyclic geometry. The homopolyatomic chalcogen dications E_8^{2+} (**4a−c**; E = S, Se, Te) are also structurally related to the eight-membered chalcogen−nitrogen rings, but the presence of two more valence electrons compared to **1** gives them an overall chairlike molecular shape with only one weak cross-ring E···E contact.[15−19]

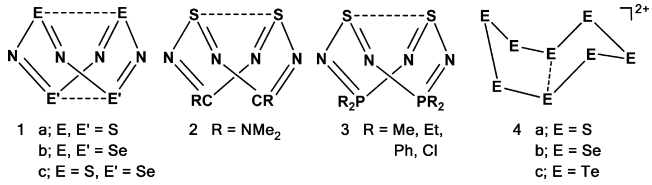

The nature of transannular interactions in **1−4** has been a matter of much debate ever since the solid state structure of S_4N_4 was first reported.[14,19−39] A simple way to rationalize the cage-like structure of S_4N_4 using molecular orbitals from extended Hückel calculations was presented by Gleiter as early as in 1970.[37] The dication $S_4N_4^{2+}$ is a planar 10 π-electron species with a doubly degenerate *e*-symmetric LUMO. Thus, the addition of two electrons to the system leads to an unstable degenerate ground state which undergoes a Jahn−Teller distortion. Of the several possible deformations that break the degeneracy, the one leading to the D_{2d} symmetric cage conformation is the most favorable, as it converts two antibonding π-type MOs to two new orbitals with a σ-type cross-ring S···S interaction. The structures of **2**, **3**, and **4** can then be derived by considering perturbations to the orbital framework of **1a** from the replacement of sulfur and nitrogen atoms with PR_2/CR and E^+/E moieties, respectively, and electrons are either removed from the cage (dithiatetrazocines) or added to it (octachalcogen dications). However, in all of these cases, the simple orbital-based model indicates that **1−4** should display classical σ bonds in place of weak chalcogen···chalcogen interactions. Clearly, such idealized Lewis models bear a resemblance to the observed molecular

Received: July 21, 2012
Published: September 24, 2012

   dx.doi.org/10.1021/ct300627p | J. Chem. Theory Comput. 2012, 8, 4249−4258

geometries, but the prediction of short chalcogen···chalcogen interactions in **1**−**4** is at variance with experimental observations.

All orbital-based bonding models are inherently qualitative in nature, and a complete theoretical description of the electronic structures of **1**−**4** naturally requires the use of more advanced techniques. Unfortunately, it has proven problematic to accurately predict the molecular geometries of **1**−**4** and, in particular, the transannular chalcogen···chalcogen interactions using the standard tools of computational chemistry. For example, the Hartree−Fock (HF) method is able to predict the bond lengths in E_4N_4 with reasonable accuracy when at least double-ζ size basis sets are used,[30] but it fails markedly with E_8^{2+} cations for which it gives a classical σ-bonded bicyclic structure irrespective of the size of the employed basis set.[29] Moreover, any attempt to include electron correlation effects in either case by means of second order perturbation theory (MP2) leads to significant overestimation of the E···E interaction.[25,29] Even density functional theory (DFT) has difficulties in providing a consistent picture of bonding in these systems, and the results are highly dependent on the chosen functional and the amount of exact exchange employed. For example, the B3LYP hybrid functional predicts the cross-ring S···S distances in dithiatetrazocines rather accurately,[21] but for no obvious reasons it overestimates those in S_4N_4 and E_8^{2+}.[25,40] On the other hand, the nonhybrid version of the same functional, namely BLYP, has considerable difficulties in reproducing the transannular interactions in E_8^{2+},[29] whereas the MPW91PW91 functional is known to provide highly accurate bond lengths even when combined with very small basis sets.[19]

On the basis of the current theoretical data for **1**−**4**, it is safe to conclude that a solid physical explanation of their weak cross-ring bonds is still lacking. Clearly the observed E···E interactions cannot be described using arguments based on orbitals alone as it would imply that the major characteristics of these systems would be portrayed even at the HF level. In addition, the short E···E distances in **1**−**4** are not a manifestation of conventional attraction between two closed shell main group centers as perturbative treatment of electron correlation is known to account for dispersion effects and many density functional methods lack them altogether. To the best of our knowledge, the only detailed, albeit preliminary, post-HF wave function based investigation of the nature of transannular bonding in any of **1**−**4** was presented by Cioslowski and Gao in 1997.[29] Their analysis of the localized MP2 orbitals of Se_8^{2+} revealed significant fractional occupancies for the formally doubly filled and empty frontier MOs. Thus, as the authors conclude, the actual wave functions of E_8^{2+} dications are "expected to possess considerable multiconfigurational character", which implies that their ground states would have a sizable singlet diradical component. Unfortunately, the natural orbital analysis was only performed for an experimentally unknown cage conformer of Se_8^{2+} (analogous to E_4N_4), and no high-level multiconfigurational or coupled cluster results capable of validating or refuting the predictions were reported due to computer hardware limitations at the time. Although no comparable data are currently available for **1**, **2**, or **3**, the possible role of diradical configurations in the wave functions of tetrachalcogen tetranitrides has been mentioned in a footnote of a recent review.[41]

The electronic structures of **1**−**4** have received renewed attention. For example, the strength of the S···S interaction in S_4N_4 was recently estimated to be on the order of typical hydrogen bonds,[28] and the electrochemical and photochemical behaviors of S_4N_4 have been the subject of several detailed and complementary investigations.[42−44] Furthermore, bonding in dithiatetrazocines has been discussed in the context of homoaromaticity[14,22] and the importance of these analyses highlighted in a *Nature Chemistry* commentary.[24] Consequently, it is of importance that an unambiguous answer to the question of the physical origin of transannular interactions in **1**−**4** is found. Hence, we have now carried out comprehensive theoretical investigations on the electronic structures of **1** and **4** using the highest possible levels of theory. Rigorous wave function analyses reveal that the ground states of these systems are very complex and contain a particularly strong correlation contribution. The presented view is the first that is able to give an all-inclusive picture of the nature of cross-ring interactions in **1** and **4**: not only does it succeed in reproducing all experimental structures but it also offers a solid explanation for the sporadic performance of different computational methods that has been reported in previous studies. The bonding in chalcogen dications E_8^{2+} is shown to pose a particularly noteworthy challenge to theory due to exceptionally strong dynamic electron correlation effects, and very high-level approaches are required in order to capture the subtleties in their electronic structure. The virtues and shortcomings of density functional theory in modeling the electronic structures of **1** and **4** are also discussed.

COMPUTATIONAL DETAILS

The geometries of E_4N_4 and E_8^{2+} (E = S, Se) were first optimized in the gas phase using D_{2d} and C_s symmetries, respectively, and different wave function based approaches: Hartree−Fock (HF), Möller−Plesset perturbation theory (MP2, MP3, and MP4),[45] complete active space without (CAS)[46] and with the second order perturbation theory correction (CASPT2),[47,48] multireference configuration interaction without (MRCISD)[49,50] and with Pople correction (MRCISD+QP),[51] quadratic configuration interaction (QCISD(T)),[52] and coupled cluster (CCSD(T)).[53] In addition to ab initio methods, density functional theory (DFT) was also used in the optimizations, and the performance of a variety of exchange correlation functionals, namely BLYP,[54,55] B3LYP,[54−56] PBEPBE,[57−59] PBE0,[57−60] M06-2X,[61] and M06-HF,[62,63] was tested both with and without the empirical DFT-D3 dispersion correction.[64]

In gas phase calculations, correlation consistent triple-ζ cc-pVTZ basis sets were used for all elements.[65−67] For S_4N_4, all calculations were also performed using the aug-cc-pVTZ basis set that includes diffuse functions which are typically necessary to describe weak correlation effects such as dispersion.[65,66] In the current case, however, augmenting the basis set had only a very minor impact on the calculated geometries while it significantly increased both the computational requirements and the CPU time. Consequently, calculations for Se_4N_4 and E_8^{2+} were performed only using the cc-pVTZ basis sets. In all post-HF methods, electrons within the largest possible halogen core were treated as frozen and excluded from the calculation of correlation effects. The only exception to this are the MRCI and CASPT2 calculations for selenium-containing species, in which case the d orbitals were also excluded from the correlation space due to software limitations.

Solid state calculations were performed for S_4N_4 and $S_8(AsF_6)_2$ using experimental X-ray structures as starting points

for geometry optimizations. For both structures, the atomic positions were fully optimized while the lattice parameters were kept fixed to ensure convergence and speed up the calculations. The Karlsruhe triple-ζ-valence + polarization (def-TZVP) basis sets were applied for S and N atoms.[68] In the case of $S_8(AsF_6)_2$, the AsF_6^- counteranions were described using slightly smaller split-valence + polarization (SVP) basis sets (see Supporting Information).[69] Monkhorst-Pack type grids of k-points in the reciprocal space were generated using shrinking factors of 4 and 2 for S_4N_4 and $S_8(AsF_6)_2$, respectively.[70] For the evaluation of the Coulomb and exchange integrals, tight tolerance factors of 8, 8, 8, 8, and 16 were used. Default optimization convergence thresholds and an extra-large integration grid for the density-functional part were applied in all calculations.

Calculations in the gas phase were performed with the Gaussian 09,[71] Molpro 2010.1,[72] and Turbomole 6.3[73] program packages, whereas all solid state calculations were done using CRYSTAL09.[74] Visualizations of molecular orbitals were done with the cross-platform molecule editor Avogadro.[75]

RESULTS AND DISCUSSION

The crystal and molecular structure of S_4N_4 has been determined on several occasions in the solid state. In the current contribution, we use the gas phase electron diffraction data of Rice et al. as a reference.[76] For Se_4N_4, high-quality crystallographic data are not available, and there are only two structure determination reports in the ICSD database. Consequently, we use average values calculated from the data for α- and β-Se_4N_4 for comparison with the theoretical predictions.[7,8] For S_8^{2+}, the high-resolution X-ray structure of the salt $S_8(AsF_6)_2$ by Passmore et al. is used as a reference,[19] while the optimized metrical parameters of Se_8^{2+} are compared with data for the dication in the salt $(Te_6^{4+})(Se_8^{2+})(AsF_6^-)_6(SO_2)$ as determined by Gillespie et al.[17]

In the crystallographic data, tetrachalcogen tetranitrides and octachalcogen dications have nearly ideal D_{2d} and C_s molecular symmetries, respectively.[4,5,7,8,15,19] For E_4N_4, there are several short (3.1−3.2 Å) E···N contacts between the four molecules in the unit cell. Similarly, short (2.7−3.3 Å) E···F contacts exist between the chalcogen dications and AsF_6^- anions in the X-ray data of both S_8^{2+} and Se_8^{2+}. This raises the important question of to what extent the short transannular interactions in Se_4N_4 and E_8^{2+} are affected by weak intermolecular and cation···anion interactions present in the crystal lattices of these compounds. A partial answer to this problem is found by comparing the electron diffraction study of S_4N_4 with the low temperature X-ray data of de Lucia and Coppens,[5] which demonstrates that the molecular structure is not significantly affected by the change in the environment; the transannular S···S contact is only moderately longer in the gas phase, 2.666(14) Å, and this could also be an effect of the temperature alone. Similar structural studies of Se_4N_4 and E_8^{2+} in the gas phase would be highly desired. However, in the former case they are precluded by the high tendency of tetraselenium tetranitride to explode violently on heating,[6] whereas in the latter case the dications are lattice stabilized and inherently unstable in the gas phase toward dissociation.[19]

Single Determinant Methods. The structures of E_4N_4 and E_8^{2+} (E = S, Se) were first calculated in the gas phase with different theoretical methods based on a single reference determinant (HF, MP*n*, QCISD(T), CCSD(T), and DFT). A summary of the results is presented in Figure 2; a full listing of optimized structural parameters is given in the Supporting Information. It is immediately evident from Figure 2 that all employed methods predict both E−N and E−E bond lengths with very good accuracy: the deviation between the calculated and the experimental data does not exceed ±0.05 Å in any case. However, a vastly different picture of the performance of different theoretical methods is obtained when the calculated values for the transannular E···E contacts are compared with the X-ray data.

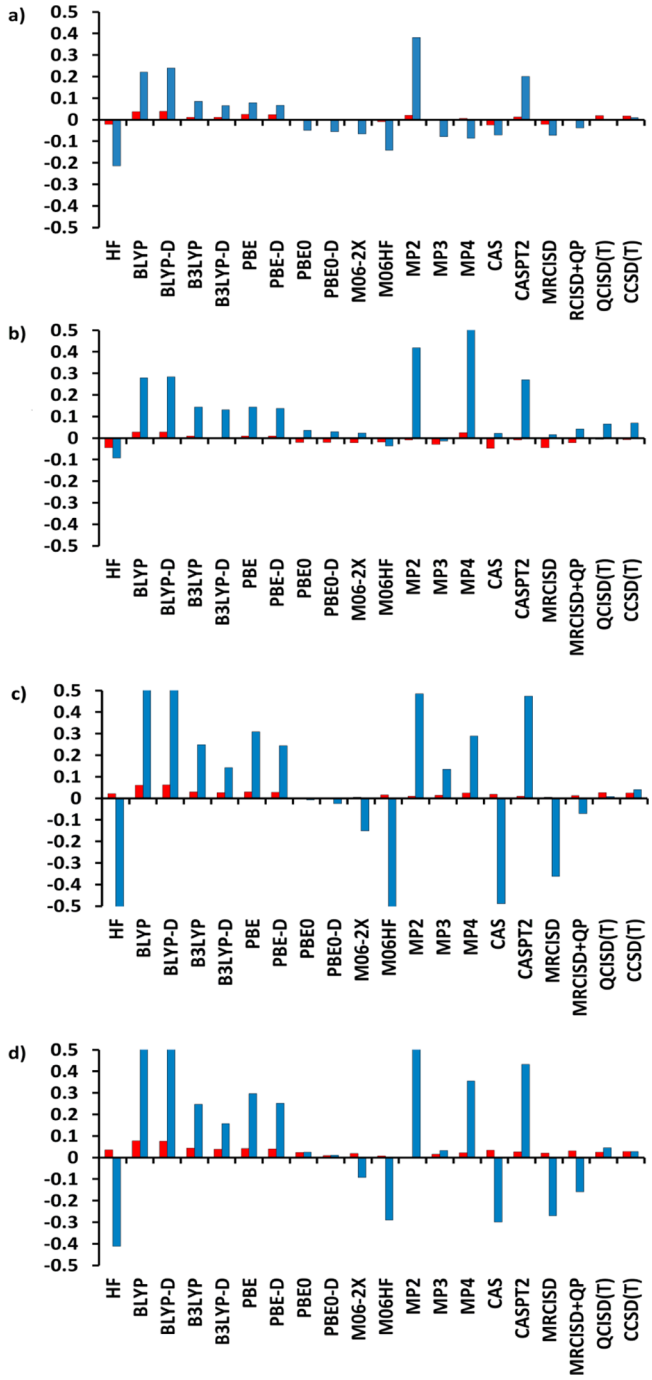

Figure 2. Deviations between the calculated and experimental bond lengths (in Ångströms) for (a) S_4N_4, (b) Se_4N_4, (c) S_8^{2+}, and (d) Se_8^{2+}. All data calculated in the gas phase. Color code: E−N and E−E bond lengths (red), E···E bond lengths (blue).

As discussed in the Introduction, the HF method underestimates the E···E contacts in E_4N_4 and particularly in E_8^{2+}, whereas MP2 predicts virtually no interaction between the two

dx.doi.org/10.1021/ct300627p | J. Chem. Theory Comput. 2012, 8, 4249−4258

chalcogen centers in either system.[25,29,30] The data in Figure 2 show that the established trends persist also when using these methods together with modern large, triple-ζ-valence-sized basis sets. Carrying out the perturbative treatment of correlation effects to the third order is found to significantly improve the calculated E···E distances in all cases, but the addition of fourth order terms again results in substantial, up to 0.5 Å, elongation of the transannular contacts. Of all the different single determinant based wave function methods employed, the QCISD(T) and CCSD(T) approaches are the only ones that show uniform performance and give geometrical parameters that are in good agreement with the experimental data.

DFT is formally a single determinant method, and hence it is natural to discuss the results obtained with different density functionals in the current context. The data in Figure 2 show a clear trend toward shorter E···E contacts when the amount of exact exchange in the functional is increased. In this sense, BLYP (no exact exchange) and M06-HF (full HF exchange) reside at the opposite ends of the spectrum and yield results close to MP2 and HF, respectively. Of all the different functionals employed, PBE0 shows the best performance, giving structural data that in most cases supersede the CCSD(T) and QCISD(T) levels of theory. The M06-2X functional, which is designed for main group systems and weak interactions, yields equally good results for E_4N_4 as PBE0, but it underestimates the E···E contact in E_8^{2+} by 0.1−0.2 Å. It is also notable from Figure 2 that the inclusion of dispersion effects to DFT via empirical correction (DFT-D) does not lead to any significant improvement of the data for tetrachalcogen tetranitrides. However, the results for E_8^{2+} cations are partially affected by the employed dispersion correction as the E···E contacts decrease roughly by 0.1 Å for both B3LYP-D and PBE-D; for the PBE0 functional, the effect of empirical dispersion correction on the E···E distance is only minimal.

As noted above, there are several short intermolecular and cation−anion interactions in the crystal structures of E_4N_4 and E_8^{2+}.[4,5,7,8,15,19] In the case of S_4N_4, the structure of the molecule has also been determined in the gas phase, and the results coincide with the solid state data, supporting the notion that secondary bonding interactions have little to no effect on the observed transannular E···E distances in tetrachalcogen tetranitrides. However, since there are no experimental gas phase structural data of E_8^{2+} available, the same conclusion cannot readily be drawn for these systems. It is entirely possible that the numerous weak anion···cation interactions present in the crystal lattice of E_8^{2+} each increase the E···E distance, in which case the structures of octachalcogen dications would be markedly dissimilar in different phases, thereby invalidating all comparisons between X-ray and computational data. In an attempt to resolve this issue, we conducted solid state geometry optimizations for $S_8(AsF_6)_2$ using the same single determinant methods as employed in the gas phase calculations (HF, B3LYP, PBE, and PBE0). For comparison, the solid state analyses were also performed for S_4N_4.

The results from solid state geometry optimizations of S_4N_4 and $S_8(AsF_6)_2$ reproduce the trends from gas phase calculations (Supporting Information). Again, HF predicts E···E distances that are very short, even shorter than that found in the gas phase, while PBE and B3LYP give mutually similar results and overestimate the transannular contacts by a small margin. The best results are obtained with the hybrid PBE0 functional that yields optimized structural parameters which are in excellent agreement with the X-ray data. We note that the solid state HF optimization of $S_8(AsF_6)_2$ failed due to convergence problems in the SCF evaluation, indicative of inherent difficulties in the theoretical method to describe the electronic structure of the dication. Although the different methods display a varying performance in modeling the key E···E contacts in S_4N_4 and S_8^{2+} in the solid state, they all incorporate the numerous short intermolecular and cation−anion interactions present in the crystal lattices of S_4N_4 and $S_8(AsF_6)_2$, respectively, which is precisely what is observed experimentally. Consequently, the solid state optimizations lend strong support to the view that secondary bonding interactions do not play a decisive role in determining the length of E···E contacts in either E_8^{2+} or E_4N_4.

Even though Figure 2 contains significantly more data points than any of the preceding computational analyses of bonding in E_4N_4 and E_8^{2+}, the observed trends are difficult to rationalize as such. The short E···E contacts predicted by HF are qualitatively in line with the wave function always being an equal mixture of covalent and ionic contributions, but its effect on molecular geometries is typically much smaller than that observed in the current case. It is also known from theory that Möller−Plesset series can display highly divergent behavior, but divergence is usually not observed until the perturbative corrections are calculated to higher orders.[77] The poorer performance of BLYP and B3LYP in comparison with PBE and PBE0 can be rationalized with the fact that the LYP correlation functional does not obey the uniform electron gas limit: a correct limiting behavior for different density functionals has recently been shown to be important for the description of different types of bonding interactions such as metal−metal and agostic bonds.[78−80] However, it is not readily apparent why the GGA and hybrid versions of the PBEPBE functional lead to very large differences in the predicted E···E distances.

Taking all of the above into account, the trends in Figure 2 can be explained by assuming that the wave functions of E_4N_4 and E_8^{2+} are dominated by "unexpectedly large electron correlation effects" as suggested initially by Cioslowski and Gao.[29] In such a case, the HF determinant is both quantitatively and qualitatively a poor approximation of the true many-electron wave function, which bodes ill for any perturbative treatment of correlation effects. In contrast, the coupled cluster and quadratic configuration interaction are known to give accurate results for many computationally difficult cases provided that at least approximate treatment of triple excitations is employed, i.e., CCSD(T) or QCISD(T).[81] Similarly, the ability of DFT to treat complex electron correlation effects is much better than that of perturbation theory and naturally depends heavily on the type of functional used in the calculations.[82] Before following this route onward and examining the performance of multideterminant methods in modeling the structures of E_4N_4 and E_8^{2+}, we investigated the composition of the calculated QCISD(T) wave functions in more detail with the help of natural orbital analysis.

Natural Orbital Analysis. Natural orbitals (NOs) are, by definition, the eigenfunctions of the one-electron density matrix and their occupancies are the eigenvalues of this matrix.[83] Their computational importance lies in the fact that CI expansions based on these orbitals typically show the fastest convergence. Furthermore, the analysis of fractionally occupied NOs makes possible a simple interpretation of correlation effects because the orbitals are localized in the region of space where the correlation error is large. NOs also provide a unique description

of the system by converging to well-defined values in the exact wave function and infinite basis set limit.[84]

NOs were calculated for the optimized geometries of E_4N_4 and E_8^{2+} at the QCISD(T) level of theory, and full numerical listings are given in the Supporting Information. The data show that there are indeed a number of NOs with notable fractional occupations (either significantly lower than 2 or higher than 0) in both E_4N_4 and E_8^{2+}. In all four systems studied, the most important fractionally occupied NOs (which correspond to the frontier MOs of these systems) are centered on the chalcogen atoms involved in the key transannular interactions, and they are either bonding (fractional occupation 1.85−1.88 e^-) or antibonding (fractional occupation 0.16−0.20 e^-) with respect to the E···E bond (see Figure 3). At first glance, this implies

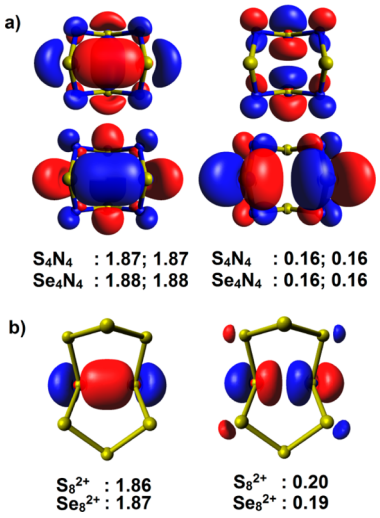

Figure 3. The most important fractionally occupied QCISD(T) natural orbitals of (a) E_4N_4 and (b) E_8^{2+} (E = S, Se) along with their occupancies (isosurface value ± 0.05).

that, in addition to the main HF determinant, HOMO−1(−2) ⇒ LUMO(+1) excited configurations make a significant contribution to the wave functions of E_4N_4 and E_8^{2+}, which would be in line with the diradical character suggested to be present in these systems. In general, single determinant methods are deemed computationally insufficient whenever the wave function contains NOs with occupancies greater than 0.10 e^-.[85]

Irrespective of the physical origin of large NO occupancies in the wave functions of E_4N_4 and E_8^{2+}, Figure 3 clearly shows that the key correlation effects in these systems involve the E···E interactions. At the HF level, orbital occupancies are either 2 or 0, which means that the E···E bonding orbitals are fully occupied and the E···E antibonding orbitals are empty. This corresponds to the picture portrayed by the idealized Lewis models **1′** and **4′**. When electron correlation is introduced, electron density is transferred from occupied to virtual orbitals, and the wave function becomes a linear combination of multiple Slater determinants, all formally excited with respect to the HF model. In E_4N_4 and E_8^{2+}, this results in significant weakening of the E···E interactions as electron density is removed from an E···E bonding orbital and transferred to an E···E antibonding orbital. Experimentally the weak transannular interactions are found to be longer in E_8^{2+} than in E_4N_4, which parallels the trend in calculated NO occupancies. The performance of different wave function based methods in modeling the E···E interactions in E_4N_4 and E_8^{2+} is then related to their ability to describe the key correlation effects, in other words, the population of the E···E bonding and antibonding orbitals. We note that the same does not hold for Kohn−Sham DFT as its formalism does not allow fractional orbital occupancies. Consequently, in DFT, electron correlation is not modeled by the reference determinant but the exchange-correlation functional and neither the role nor origin of different correlation effects can be determined directly from the optimized Kohn−Sham orbitals.[82]

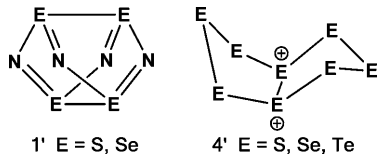

The NO occupations calculated for E_4N_4 and E_8^{2+} at the QCISD(T) level are exceptionally large. Typically, values less than 0.05 e^- are observed for molecular systems that are well described by a single Slater determinant, such as the water molecule. However, the good performance of QCISD(T) in reproducing the geometries of E_4N_4 and E_8^{2+} allows us to conclude that the observed occupancies at this level must be sufficiently close to the values at the exact wave function limit. Furthermore, we expect that any increase of the basis set size would only lead to small quantitative changes to the calculated NO occupancies, with the fundamental, qualitative behavior being virtually unaltered.[84] Hence, it is left to determine if the observed correlation is primarily static or dynamic in nature. Regardless of the answer, it is evident that the electron correlation effects in these systems are quite unique and not primarily of dispersion-type, as dispersion is a purely attractive phenomenon. This is also in line with the DFT results discussed above that showed only very minor improvements when the functionals were augmented with an empirical dispersion correction.

Multideterminant Methods. In order to determine the nature of electron correlation effects in E_4N_4 and E_8^{2+}, their geometries and wave functions were re-examined using multideterminant methods that build upon the complete active space formalism. As a first approximation, minimum-type active spaces that consist of the most important fractionally occupied NOs in the QCISD(T) wave functions were employed (Figure 3). This corresponds to CAS-[4,4] and CAS-[2,2] wave functions for E_4N_4 and E_8^{2+}, respectively.

A summary of the optimized structures of E_4N_4 and E_8^{2+} at CAS, CASPT2, MRCISD, and MRCISD+QP levels is presented in Figure 2; full listings of optimized structural parameters are given in the Supporting Information. It is immediately evident from Figure 2 that the use of a multideterminant wave function results in no significant changes to the calculated E−N and E−E bond lengths, which are once again predicted with excellent accuracy with different methods. However, the data for the transannular E···E interactions show some interesting trends.

Geometry optimizations using a CAS-type wave function yield vastly different results for E_4N_4 and E_8^{2+}. For E_4N_4, the optimized geometries are in good qualitative agreement with the experimental data, whereas for E_8^{2+} the experimental E···E distance is significantly (up to 0.5 Å) longer than that given by the CAS method. Clearly the employed CAS wave function gives only a very poor description of electron correlation effects

dx.doi.org/10.1021/ct300627p | J. Chem. Theory Comput. 2012, 8, 4249−4258

in E_8^{2+}. It is therefore not entirely surprising that the observed trend remains virtually unchanged when dynamic electron correlation effects are treated with the MRCISD method. However, a noticeable improvement in the optimized E···E distance of E_8^{2+} is observed with MRCISD+QP that takes into account dynamic four-electron correlation effects in an ad hoc manner (Pople correction). In contrast to the MRCI and CAS data, the CASPT2 method is found to significantly overestimate the E···E distances in both E_4N_4 and in E_8^{2+}, though the error is considerably smaller for the former systems.

Taken as a whole, the multideterminant data in Figure 2 demonstrate that electron correlation effects in E_4N_4 and in E_8^{2+} must have a different explanation. In the case of E_4N_4, the exact wave function can be adequately approximated with only a very few reference determinants, i.e., CAS-[4,4], indicative of static electron correlation and multiconfigurational character associated with the two E···E interactions. However, the same is not true for E_8^{2+}, as all attempts to describe the important electron correlation effects inferred from the QCISD(T) NO occupancies with a minimum active space CAS approach led only to slight improvement of the results over the HF solution. This in turn suggests that the wave functions of octachalcogen dications are not dominated by static electron correlation effects but instead governed mostly by dynamic correlation. Consequently, of all the multideterminant methods employed, only MRCISD+QP is able to yield adequate structural data for E_8^{2+} since it treats dynamic correlation in a roughly equivalent manner to a QCISD (or CCSD) calculation and therefore reaches the minimum level of theory needed to get a reasonable description of the key correlation effects.

The presented view of electron correlation effects in E_4N_4 and in E_8^{2+} and how they relate to the transannular E···E interactions is further supported by CAS geometry optimizations employing active spaces of progressively increasing size: no significant changes in the E ···E distance or in the NO occupancies are observed in these calculations. For E_4N_4, the NO occupancies at the CAS level of theory are qualitatively in accord with the QCISD(T) results irrespective of the size of the active space. However, for E_8^{2+} the CAS method consistently yields fractional occupancies that are significantly less than the QCISD(T) results, only around 0.06−0.07 e^- for the E···E antibonding orbital. In this case, only a third of the correlation effects can be assigned to a single HOMO−1 ⇒ LUMO type excited configuration, and a large and balanced set of determinants is needed to get an accurate description of transannular E···E bonding in E_8^{2+}. This is achieved much more conveniently at the QCISD(T) and CCSD(T) levels than using a CAS-type wave function.

The importance of the excitation level (single, double or triple) for the description of E···E bonding in E_8^{2+} was examined in more detail by carrying out CI and CC level optimizations for S_8^{2+}. When using the CISD method, the optimized S···S interaction is 2.362 Å, which is only 0.1 Å longer than the HF value. This result can be contrasted with the optimized MRCISD distance of 2.508 Å, which shows that the inclusion of a second reference determinant lengthens the S···S bond by roughly the same amount. However, the MRCISD result still falls 0.4 Å short from the experimental value. Inclusion of four-electron correlation effects for size-consistency with either QCISD, CCSD, or Pople correction (MRCISD+QP) lengthens the S···S distance to 2.572, 2.627, and 2.791 Å, respectively. Hence, the disconnected double excitations play a major role in elongating the key E···E interaction, which is also reflected in the occupancy of the S···S antibonding NO that increases to 0.13 and 0.11 e^- at the QCISD and CCSD levels, respectively. An equally significant change is observed in the single determinant results when the contribution of triple excitations is taken into account: at the QCISD(T) level, the optimized S···S distance is 2.866 Å and the corresponding antibonding NO occupancy is 0.20 e^-. However, it needs to be noted that an approximate treatment of triple excitations in QCI and CC theories tends to overestimate their importance, and including the T term explicitly in the cluster operator is expected to yield results in between the SD and SD(T) values. In light of the above data, the sporadic performance of perturbation theory and different density functionals in describing the electronic structure of E_8^{2+} can be understood. The HF wave function is indeed a very poor approximation of these systems, and electron correlation effects cannot anymore be treated as a perturbation to the reference wave function. Similarly, not all density functionals show sufficient accuracy to describe correlation effects that with the wave function methods involve triple (and higher) excitations.

Coming back to the earlier investigations of the origin of E···E bonding in E_4N_4 and E_8^{2+}, the conclusion of large electron correlation effects in E_8^{2+}, as reached initially by Cioslowski and Gao,[29] appears to be fully correct. Nevertheless, the present analyses clearly show that these correlation effects cannot be described with a CAS wave function that has only a few determinants and that the large fractional NO occupancies and, consequently, the long E···E bonds arise from complex electron correlation effects, necessitating the use of a wave function with a large number of excited determinants. In agreement with this interpretation, the QCISD(T) NOs calculated for E_8^{2+} show multiple orbitals with fractional occupancies that are slightly higher (1.85−1.90 e^-) or lower (0.05−0.10 e^-) than the two key NOs depicted in Figure 3 (see also Supporting Information). In addition to Cioslowski and Gao, Passmore et al. have previously investigated the electronic structure of E_8^{2+} in great detail.[19] However, their analyses were based on DFT, which does not allow easy examination of the origin of different correlation effects. Consequently, the conclusions reached by Passmore et al. on the basis of total electron density analyses are justified, but the difficulties in obtaining accurate theory-based structural data for E_8^{2+} lie more in the complexity of their wave function and not in the flatness of the potential energy surface, though it also plays a role in the overall picture.

As already noted above, the electron correlation effects in E_4N_4 differ from that in E_8^{2+}. The fractional NO occupancies can in this case be qualitatively described with a limited number of HOMO−1(−2) ⇒ LUMO(+1) type excited determinants, which supports the idea of singlet diradical character in these systems. However, a proper treatment of dynamic correlation effects is still necessary to obtain a quantitatively accurate description of their electronic structure. This can readily be seen when comparing the results at CAS, MRCISD, and MRCISD+QP levels: the optimized E···E distances are virtually identical for CAS and MRCISD, whereas the data at the MRCISD+QP level are closer to the CCSD(T) value. Consequently, the effect of disconnected double (and higher) excitations to the E···E interaction is much greater than that of single and double excitations. The same conclusion can be reached from the CASPT2 data: at this level, the E−N bonds are predicted in good agreement with the experimental values, but the E···E distances are overestimated significantly, albeit not nearly as much as the conventional MP2 is. In agreement with

the trend in optimized geometrical parameters, the CASPT2 wave functions for E_4N_4 contain several doubly external configurations with coefficients greater than 0.05, whereas there is only a handful of them at the MRCISD level. Clearly the perturbative treatment of electron correlation effects overestimates the importance of double excitations and leads to fractional NO occupancies that are too high and, hence, to E···E distances that are far too long.

An analysis of the CAS wave functions for E_4N_4 shows that the combined weight of configurations involving single and double excitations from the E···E bonding orbitals to the E···E antibonding orbitals is roughly 9% as calculated from the CI vector coefficients. This does not give a direct estimate of the overall diradical character, as the excited configurations involve both of the E···E interactions, giving the molecules an overall tetraradical nature. A rough approximation (and an upper estimation) of diradical character within each E···E interaction can, however, be obtained from NO occupancies determined at the CAS level. In a perfect diradical, there are two frontier orbitals each occupied by a single electron.[86−88] Thus, an orbital occupancy of 0.10 e^- in E_4N_4 translates to a diradical character of approximately 10% per E···E bond (cf. 16% for ozone at the full valence CAS level). This is clearly a non-negligible amount, but it is still less than what can be described accurately by using the infinite-order CC and QCI approaches. In a similar fashion, almost any of the modern (GGA or hybrid) functionals will yield reasonable results for main group systems with a small to medium amount of diradical character, the actual performance in each case being determined not only by the identity of the density functional but also by the amount of exact exchange used.[82] A similar analysis of CAS NO occupation numbers for E_8^{2+} gives an upper estimate of 6% diradical character within the E···E bond, which is in agreement with the more important role of dynamic electron correlation effects in these systems.

The last theoretical evidence in support of multiconfigurational character in E_4N_4 comes from calculations probing spin states other than the singlet ground state. If the wave functions of E_4N_4 have noticeable tetraradical character, the energy difference between the singlet state and the first excited quintet state (with four truly unpaired electrons) is expected to be rather small. However, the high-spin wave function for a quintet state is not multiconfigurational and can be qualitatively described with a single Slater determinant. Consequently, a UHF optimization for S_4N_4 in the quintet state yields a minimum at 45 kJ mol^{-1} *lower* in energy than the singlet ground state. This is an excellent illustration of how poorly the HF wave function actually describes the electronic structure of singlet E_4N_4 even though the only noticeable failure in geometry optimization at this level is the slight underestimation of the E···E distance. At the PBE0 level of theory, the quintet state is predicted to be 210 kJ mol^{-1} *higher* in energy than the singlet. Thus, when all important electron correlation effects are appropriately accounted for, the ordering of the states is correct. However, the calculated adiabatic singlet-quintet energy gap is still atypically small and indicative of multiconfigurational character in the system. We note that, at the HF level, the triplet wave function for S_8^{2+} is also lower in energy than the singlet, but the energy difference between the two states is only 8 kJ mol^{-1}. This is fully in line with the conclusion of much smaller multiconfigurational character in E_8^{2+} as compared to E_4N_4.

Bonding Analysis. Having determined that the electronic structures of E_4N_4 and E_8^{2+} can be accurately modeled using the PBE0 hybrid functional, the corresponding Kohn−Sham determinants (and the total electron densities that they give rise to) were subjected to natural bond orbital (NBO), atoms in molecules (AIM), and electron localization function (ELF) analyses to obtain further insight to transannular E···E bonding.

Passmore et al. have recently published a thorough NBO analysis of E_8^{2+} dications using the B3PW91 density functional.[19] They found that representing the Kohn−Sham determinant in terms of localized electron-pair units reproduces the classical bonding picture in **4′**. However, their results also showed significant departures from the Lewis model as the total occupancy of non-Lewis type valence NBOs was found to be 1.8 e^- in S_8^{2+} (1.5 in Se_8^{2+}). A further analysis revealed that approximately one-half of these "delocalization corrections" to the zeroth-order natural Lewis structure originate from the transfer of sulfur lone pair electrons to the transannular E−E antibonding NBO. This view of bonding in E_8^{2+} is in excellent agreement with our conclusions drawn from the examination of natural orbitals.

The NBO procedure yields a very similar picture of bonding in E_4N_4 as obtained for E_8^{2+} (see Supporting Information). The zeroth-order natural Lewis structure corresponds to the classical description given in **1′** (though with localized charges and single bonds), but the non-Lewis type valence NBOs again display high occupancies which total to 2.2 e^- for S_4N_4 (2.0 for Se_4N_4). Most notably, in S_4N_4 the transannular E−E antibonding NBOs are occupied by 0.7 e^- each (0.6 in Se_4N_4), with delocalizations coming primarily from the nitrogen lone pair NBOs. These results show that for the same chalcogen E, the occupancy of the E−E antibonding NBO is lower in E_4N_4 than in E_8^{2+}, which reproduces the trend in natural orbital occupation numbers (see above). The calculated Wiberg bond indices for the transannular E···E bonds further corroborate this picture and yield higher values for E_4N_4 (e.g., 0.41 in S_4N_4) than for the corresponding E_8^{2+} (e.g., 0.26 in S_8^{2+}).

An AIM analysis of the total electron densities of E_8^{2+} dications has previously been conducted by Passmore et al.[19] The acquired data show that a bond critical point is indeed found for the transannular E···E interaction, and it is characterized by small values of both the electron density ρ (0.04 au for S_8^{2+}) and its Laplacian $\nabla\rho^2$ (0.04 au for S_8^{2+}). This indicates that the bonding is rather weak and that it shares features typically associated with closed-shell interactions. Similar results have been presented for the S···S bonds in S_4N_4 (ρ = 0.06 au; $\nabla\rho^2$ = 0.05 au) by Bader et al. although their calculations were done at the Hartree−Fock level and using much smaller basis sets.[32] However, our analyses of the PBE0/cc-pVTZ electron densities yielded bond critical point properties which are in good qualitative and quantitative agreement with the prior published data (Supporting Information). These results are supported by the analysis of the electron localization function for E_4N_4 and E_8^{2+} (Figure 4; Supporting Information), which reveals that there are no disynaptic V(E,E) bond basins within the transannular E···E interactions. However, a visualization of the ELFs (see Figure 4) demonstrates that in E_4N_4, the monosynaptic lone pair basins at the chalcogen atoms are highly polarized toward the transannular bonding region, whereas in E_8^{2+} they have a much more spherical shape. A comparison of the calculated ELF basin properties between E_4N_4 and E_8^{2+} shows the average population of the

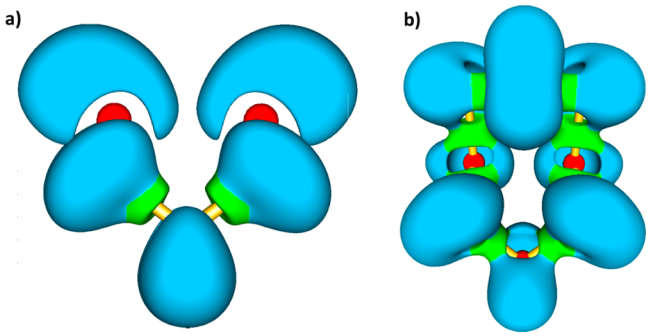

Figure 4. The electron localization functions of (a) S_4N_4 and (b) S_8^{2+} (isosurface value 0.7). Color code: core (red), monosynaptic (blue), disynaptic (green).

monosynaptic lone pair basins to be significantly smaller for the former (around 3.5 and 4.0 e^- for S_4N_4 and S_8^{2+}), which is in agreement with the different nature of correlation effects in these systems.

CONCLUSIONS

The nature of *intramolecular* chalcogen···chalcogen interactions in tetrachalcogen tetranitrides, E_4N_4, and octachalcogen dications, E_8^{2+} (E = S, Se), was studied theoretically with different ab initio methods and density functionals. Natural orbitals analysis at the quadratic configuration interaction level revealed that the E···E distances in E_4N_4 and E_8^{2+} are elongated from typical E−E single bond lengths due to surprisingly strong and complex electron correlation effects. Specifically, the wave functions of these molecules and cations contain a notable contribution from excited determinants in which the formally empty E−E antibonding orbitals are doubly occupied. In E_4N_4, the correlation effects can be described with only a few configurations involving the key orbitals at the E−E bond. Consequently, these systems are dominated by static electron correlation, and they have singlet diradical character associated with each E···E interaction. In contrast, the dications E_8^{2+} can only be described theoretically with a wave function that contains a very large number of determinants to capture dynamic correlation effects associated with disconnected double and higher excitations.

The results of the present study clearly demonstrate that once the important correlation effects are treated at an appropriate level, computational methods are able to model the electronic and molecular structures of E_4N_4 and E_8^{2+} to a very high degree. The conducted bonding analyses also offer a rationale for the difficulties reported in previous theoretical investigations, and results from solid state geometry optimizations strongly support the view that secondary bonding interactions do not affect the geometries of E_8^{2+} to any significant degree, vindicating a comparison of gas phase calculations with the X-ray crystallographic data. Of all the wave function based methods employed, CCSD(T) and QCISD(T) show the best and uniform performance; for E_4N_4, MRCISD provides an alternative method for obtaining an equally accurate description of their electronic structures. The ability of different density functionals to describe E_4N_4 and E_8^{2+} depends on the identity of the functional and, in particular, the amount of exact exchange used in its construction. The combination of PBEPBE functional with 25% of exact exchange, namely PBE0, is superior to all other functionals used and even supersedes those which are explicitly parametrized for the description of weak interactions.

As a whole, the current investigation succeeds in finding an unambiguous answer to the question of the nature of transannular interactions in E_4N_4 and E_8^{2+}. These interactions originate from covalent (orbital-based) bonding, but they are significantly weakened by electron correlation. Though not a topic of this study, we expect that a similar description of the physical basis of chalcogen···chalcogen interactions holds at least for the dithiatetrazocines **2** and **3** due to their structural and chemical relationship to E_4N_4, but possibly also for other chalcogen systems with similar cage-like structures. It needs to be stressed that the description of bonding in E_4N_4 is unique and fundamentally different from, for example, dispersion that typically plays a major role in weak *intermolecular* chalcogen···chalcogen contacts. In this respect, a better reference point for the discussed transannular interactions is offered by a weak exchange-coupling of two radical species via overlap of their singly occupied molecular orbitals. This interpretation is in agreement with the multiconfigurational nature of E_4N_4 and the fact that at the Hartree−Fock level the high-spin quartet and triplet states represent the global minima for E_4N_4 and E_8^{2+}, respectively.

ASSOCIATED CONTENT

Supporting Information

Optimized structures, QCISD(T) natural orbital occupation numbers, numeric results from NBO, AIM and ELF analyses as well as full computational details for solid state calculations. This material is available free of charge via the Internet at http://pubs.acs.org

AUTHOR INFORMATION

Corresponding Author

*E-mail: heikki.m.tuononen@jyu.fi (H.M.T.), chivers@ucalgary.ca (T.C.). Fax: +358-14-260-2501 (H.M.T.), +1-403-289-9488 (T.C.).

Notes

The authors declare no competing financial interest.

ACKNOWLEDGMENTS

Financial support from the University of Jyväskylä, the Academy of Finland (A.J.K and H.M.T) and the Technology Industries of Finland Centennial Foundation (H.M.T) is gratefully acknowledged. We also thank CSC - the IT Centre for Science Ltd for providing computational resources to this project.

REFERENCES

(1) *Handbook of Chalcogen Chemistry: New Perspectives in Sulfur, Selenium and Tellurium*; Devillanova, F. A., Ed.; RSC Publishing: Cambridge, U. K., 2007; pp 381−416.
(2) Gregory, M. *J. Pharm* **1835**, *21*, 315.
(3) Clark, D. *J. Chem. Soc.* **1952**, 1615.
(4) Sharma, B. D.; Donohue, J. *Acta Crystallogr.* **1963**, *16*, 891.
(5) DeLucia, M. L.; Coppens, P. *Inorg. Chem.* **1978**, *17*, 2336.
(6) Jander, J.; Doetsch, V. *Angew. Chem.* **1958**, *70*, 704.
(7) Bärnighausen, H.; von Volkmann, T.; Jander, J. *Acta Crystallogr.* **1966**, *21*, 571.
(8) Folkerts, H.; Neumüller, B.; Dehnicke, K. *Z. Anorg. Allg. Chem.* **1994**, *620*, 1011.
(9) Maaninen, A.; Laitinen, R. S.; Chivers, T.; Pakkanen, T. A. *Inorg. Chem.* **1999**, *38*, 3450.

(10) Ernest, I.; Holick, W.; Rihs, G.; Schomburg, D.; Shoham, G.; Wenkert, D.; Woodward, R. B. *J. Am. Chem. Soc.* **1981**, *103*, 1540.
(11) Burford, N.; Chivers, T.; Codding, P. W.; Oakley, R. T. *Inorg. Chem.* **1982**, *21*, 982.
(12) Burford, N.; Chivers, T.; Richardson, J. F. *Inorg. Chem.* **1983**, *22*, 1482.
(13) Chivers, T.; Edwards, M.; Parvez, M. *Inorg. Chem.* **1992**, *31*, 1861.
(14) Chivers, T.; Hilts, R. W.; Jin, P.; Chen, Z.; Lu, X. *Inorg. Chem.* **2010**, *49*, 3810.
(15) Davies, C. G.; Gillespie, R. J.; Park, J. J.; Passmore, J. *Inorg. Chem.* **1971**, *10*, 2781.
(16) McMullan, R. C.; Prince, D. J.; Corbett, J. D. *Inorg. Chem.* **1971**, *10*, 1971.
(17) Collins, M. J.; Gillespie, R. J.; Sawyer, J. F. *Acta Crystallogr.* **1988**, *C44*, 405.
(18) Beck, J.; Muller-Buschbaum, K. *Z. Anorg. Allg. Chem.* **1997**, *623*, 409.
(19) Cameron, T. S.; Deeth, R. J.; Dionne, I.; Du, H.; Jenkins, H. D. B.; Krossing, I.; Passmore, J.; Roobottom, H. K. *Inorg. Chem.* **2000**, *39*, 5614.
(20) Millefiori, S.; Millefiori, A.; Granozzi, G. *Inorg. Chim. Acta* **1984**, *90*, L55.
(21) Chung, G.; Lee, D. *Bull. Korean Chem. Soc.* **2000**, *21*, 300.
(22) Zhang, Q.; Yue, S.; Lu, X.; Chen, Z.; Huang, R.; Zheng, L.; Schleyer, P.; von, R. *J. Am. Chem. Soc.* **2009**, *131*, 9789.
(23) Jacobsen, H.; Ziegler, T.; Chivers, T.; Vollmerhaus, R. *Can. J. Chem.* **1994**, *72*, 1582.
(24) Rzepa, H. S. *Nature Chem.* **2009**, *1*, 510.
(25) Chung, G.; Lee, D. *J. Mol. Struct.: THEOCHEM* **2002**, *582*, 85.
(26) Bridgeman, A. J.; Cavigliasso, G.; Ireland, L. R.; Rothery, J. *J. Chem. Soc., Dalton Trans.* **2001**, 2095.
(27) Scherer, W.; Spegler, M.; Pederson, B.; Tafipolsky, M.; Hieringer, W.; Reinhard, B.; Downs, A. J.; McGrady, G. S. *Chem. Commun.* **2000**, 635.
(28) Contreras-García, J.; Johnson, E. R.; Keinan, S.; Chaudret, R.; Piquemal, J.-P.; Beratan, D. N.; Yang, W. *J. Chem. Theory Comput.* **2011**, *7*, 625.
(29) Cioslowski, J.; Gao, X. *Int. J. Quantum Chem.* **1997**, *65*, 609.
(30) Suontamo, R. J.; Laitinen, R. S. *J. Mol. Struct.: THEOCHEM* **1995**, *358*, 55.
(31) Brown, A. S.; Smith, V. H., Jr. *J. Chem. Phys.* **1993**, *99*, 1837.
(32) Tang, T. H.; Bader, R. F. W.; MacDougall, P. J. *Inorg. Chem.* **1985**, *24*, 2047.
(33) Findlay, R. H.; Palmer, M. H.; Downs, A. J.; Egdell, R. G.; Evans, R. *Inorg. Chem.* **1980**, *19*, 1307.
(34) Salahub, D. R.; Messmer, R. P. *J. Chem. Phys.* **1976**, *64*, 2039.
(35) Gopinathan, M. S.; Whitehead, M. A. *Can. J. Chem.* **1975**, *53*, 1343.
(36) Tanaka, K.; Yamabe, T.; Tachibana, A.; Kato, H.; Fukui, K. *J. Phys. Chem.* **1978**, *82*, 2121.
(37) Gleiter, R. *J. Chem. Soc. A* **1970**, 3174.
(38) Cassoux, P.; Labarre, J.-F.; Glemser, O. *J. Mol. Struct.* **1972**, *13*, 405.
(39) Baird, N. C. *J. Comput. Chem.* **1984**, *5*, 35.
(40) Krossing, I. *Top. Curr. Chem.* **2003**, *230*, 79.
(41) Breher, F. *Coord. Chem. Rev.* **2007**, *251*, 1007.
(42) Boeré, R. T.; Chivers, T.; Roemmele, T. L.; Tuononen, H. M. *Inorg. Chem.* **2009**, *48*, 7294.
(43) Pritchina, E. A.; Gritsan, N. P.; Bally, T.; Zibarev, A. V. *Inorg. Chem.* **2009**, *48*, 4075.
(44) Pritchina, E. A.; Terpilovskaya, D. S.; Tsentalovich, Y. P.; Platz, M. S.; Gritsan, N. P. *Inorg. Chem.* **2012**, *51*, 4747.
(45) Møller, C.; Plesset, M. S. *Phys. Rev.* **1934**, *46*, 618.
(46) Roos, B. E.; Taylor, P. R.; Siegbahn, P. E. M. *Chem. Phys.* **1980**, *48*, 157.
(47) Andersson, K.; Malmqvist, P.-Å.; Roos, B. O. *J. Chem. Phys.* **1992**, *96*, 1218.
(48) Celani, P.; Werner, H.-J. *J. Chem. Phys.* **2000**, *112*, 5546.
(49) Werner, H.-J.; Knowles, P. J. *J. Chem. Phys.* **1988**, *89*, 5803.
(50) Knowles, P. J.; Werner, H.-J. *Phys. Lett.* **1988**, *145*, 514.
(51) Pople, J.; Seeger, R. *Int. J. Quantum Chem.* **1977**, *12*, 149.
(52) Pople, J. A.; Head-Gordon, M.; Raghavachari, K. *J. Chem. Phys.* **1987**, *87*, 5968.
(53) Raghavachari, K.; Trucks, G. W.; Pople, J. A.; Head-Gordon, M. *Chem. Phys. Lett.* **1989**, *157*, 479.
(54) Becke, A. D. *Phys. Rev. A: At., Mol., Opt. Phys.* **1988**, *38*, 3098.
(55) Lee, C.; Yang, W.; Parr, R. G. *Phys. Rev. B: Condens. Matter Mater. Phys.* **1988**, *37*, 785.
(56) Stephens, P. J.; Devlin, F. J.; Chabalowski, C. F.; Frisch, M. J. *J. Phys. Chem.* **1994**, *98*, 11623.
(57) Perdew, J. P.; Burke, K.; Ernzerhof, M. *Phys. Rev. Lett.* **1996**, *77*, 3865.
(58) Perdew, J. P.; Burke, K.; Ernzerhof, M. *Phys. Rev. Lett.* **1997**, *78*, 1396.
(59) Perdew, J. P.; Ernzerhof, M.; Burke, K. *J. Chem. Phys.* **1996**, *105*, 9982.
(60) Adamo, C.; Barone, V. *J. Chem. Phys.* **1999**, *110*, 6158.
(61) Zhao, Y.; Truhlar, D. G. *Theor. Chem. Acc.* **2008**, *120*, 215.
(62) Zhao, Y.; Truhlar, D. G. *J. Phys. Chem. A* **2006**, *110*, 5121.
(63) Zhao, Y.; Truhlar, D. G. *J. Phys. Chem. A* **2006**, *110*, 13126.
(64) Grimme, S; Antony, J.; Ehrlich, S.; Krieg, H. *J. Chem. Phys.* **2010**, *132*, 154104.
(65) Dunning, T. H., Jr. *J. Chem. Phys.* **1989**, *90*, 1007.
(66) Woon, D. E.; Dunning, T. H., Jr. *J. Chem. Phys.* **1993**, *98*, 1358.
(67) Wilson, A. K.; Woon, D. E.; Peterson, K. A.; Dunning, T. H., Jr. *J. Chem. Phys.* **1999**, *110*, 7667.
(68) Schäfer, A.; Huber, C.; Ahlrichs, R. *J. Chem. Phys.* **1994**, *100*, 5829.
(69) Schaefer, A.; Horn, H.; Ahlrichs, R. *J. Chem. Phys.* **1992**, *97*, 2571.
(70) Monkhorst, H. J.; Pack, J. D. *Phys. Rev. B* **1976**, *13*, 5188.
(71) Frisch, M. J.; Trucks, G. W.; Schlegel, H. B.; Scuseria, G. E.; Robb, M. A.; Cheeseman, J. R.; Scalmani, G.; Barone, V.; Mennucci, B.; Petersson, G. A.; Nakatsuji, H.; Caricato, M.; Li, X.; Hratchian, H. P.; Izmaylov, A. F.; Bloino, J.; Zheng, G.; Sonnenberg, J. L.; Hada, M.; Ehara, M.; Toyota, K.; Fukuda, R.; Hasegawa, J.; Ishida, M.; Nakajima, T.; Honda, Y.; Kitao, O.; Nakai, H.; Vreven, T.; Montgomery, J. A., Jr.; Peralta, J. E.; Ogliaro, F.; Bearpark, M.; Heyd, J. J.; Brothers, E.; Kudin, K. N.; Staroverov, V. N.; Kobayashi, R.; Normand, J.; Raghavachari, K.; Rendell, A.; Burant, J. C.; Iyengar, S. S.; Tomasi, J.; Cossi, M.; Rega, N.; Millam, J. M.; Klene, M.; Knox, J. E.; Cross, J. B.; Bakken, V.; Adamo, C.; Jaramillo, J.; Gomperts, R.; Stratmann, R. E.; Yazyev, O.; Austin, A. J.; Cammi, R.; Pomelli, C.; Ochterski, J. W.; Martin, R. L.; Morokuma, K.; Zakrzewski, V. G.; Voth, G. A.; Salvador, P.; Dannenberg, J. J.; Dapprich, S.; Daniels, A. D.; Farkas, Ö.; Foresman, J. B.; Ortiz, J. V.; Cioslowski, J.; Fox, D. J. *Gaussian 09*, revision C.1; Gaussian, Inc.: Wallingford, CT, 2009.
(72) Werner, H.-J.; Knowles, P. J.; Knizia, G.; Manby, F. R.; Schütz, M.; et al. *MOLPRO*, version 2010.1. See http://www.molpro.net (accessed Sept. 2012).
(73) *TURBOMOLE V6.4 2012*; University of Karlsruhe and Forschungszentrum Karlsruhe GmbH: Karlsruhe, Germany, 1989–2007; TURBOMOLE GmbH: Karlsruhe, Germany, 2007. Available from http://www.turbomole.com.
(74) Dovesi, R.; Saunders, V. R.; Roetti, R.; Orlando, R.; Zicovich-Wilson, C. M.; Pascale, F.; Civalleri, B.; Doll, K.; Harrison, N. M.; Bush, I. J.; D'Arco, P.; Llunell, M. *CRYSTAL09 User's Manual*; University of Torino: Torino, Italy, 2009.
(75) *Avogadro*, version 1.0.3. Available from: http://avogadro.openmolecules.net/ (accessed Sept. 2012).
(76) Almond, M. J.; Forsyth, G. A.; Rice, D. A.; Downs, A. J.; Jeffery, T. L.; Hagen, K. *Polyhedron* **1989**, *8*, 2631.
(77) Olsen, J.; Jørgensen, P.; Helgaker, T.; Christiansen, O. *J. Chem. Phys.* **2000**, *112*, 9736.
(78) Zhao, S.; Li, Z.-H.; Wang, W.-N.; Liu, Z.-P.; Fan, K.-N.; Xie, Y.; Schaefer, H. F. *J. Chem. Phys.* **2006**, *124*, 184102.

(79) Paier, J.; Marsman, M.; Kresse, G. *J. Chem. Phys.* **2007**, *127*, 024103.
(80) Pantazis, D. A.; McGrady, J. E.; Maseras, F.; Etienne, M. *J. Chem. Theory Comput.* **2007**, *3*, 1329.
(81) Bally, T.; Borden, W. T. In *Reviews of Computational Chemistry*; Lipkowitz, K. B., Boyd, D. B., Eds.; VCH: New York, 1999; pp 37−39.
(82) Cremer, D. *Mol. Phys.* **2001**, *99*, 1899.
(83) Löwdin, P.-O. *Phys. Rev.* **1955**, *97*, 1474.
(84) Gordon, M. S.; Schmidt, M. W.; Chaban, G. M.; Glaesemann, K. R.; Steevens, W. J.; Gonzalez, C. *J. Chem. Phys.* **1999**, *110*, 4199.
(85) Gordon, M. S.; Schmidt, M. W. *Annu. Rev. Phys. Chem.* **1998**, *49*, 233.
(86) Flynn, C.; Michl, J. J. *Am. Chem. Soc.* **1974**, *96*, 3280.
(87) Dohnert, D.; Koutecky, J. *J. Am. Chem. Soc.* **1980**, *102*, 1789.
(88) Bonacic-Koutecky, V.; Koutecky, J.; Michl, J. *Angew. Chem., Int. Ed. Engl.* **1987**, *26*, 170.